PROCEEDINGS OF THE
AMERICAN MATHEMATICAL SOCIETY
Volume 144, Number 10, October 2016, Pages 4205–4219
http://dx.doi.org/10.1090/proc/12678
Article electronically published on June 10, 2016

FINITE CYCLICITY OF SLOW-FAST DARBOUX SYSTEMS WITH A TWO-SADDLE LOOP

MARCIN BOBIEŃSKI AND LUBOMIR GAVRILOV

(Communicated by Walter Van Assche)

Abstract. We prove that the cyclicity of a slow-fast integrable system of Darboux type with a double heteroclinic loop is finite and uniformly bounded.

1. Introduction

Let $\mathcal{F}_\varepsilon$ be an analytic family of analytic real plane foliations (or vector fields), depending on a small parameter ε, and having for all $\varepsilon > 0$ a bounded period annulus (a nest of periodic orbits) Π_ε. We shall suppose, moreover, that $\mathcal{F}_\varepsilon$ is a Darboux integrable plane foliation, and $\mathcal{F}_0$ has a curve of singular points (slow manifold), as in Figure 1.1. The family $\mathcal{F}_\varepsilon$ will be referred to as a *slow-fast integrable system of Darboux type*.

Consider a further multi-parameter analytic deformation $\mathcal{F}_{\varepsilon,\delta}$ of $\mathcal{F}_\varepsilon$, and denote by $Z(\varepsilon) = Cycl(\mathcal{F}_{\varepsilon,\delta}, \bar{\Pi}_\varepsilon)$ the maximal number of limit cycles which bifurcate from the closure $\bar{\Pi}_\varepsilon$ for sufficiently small $\|\delta\|$. The number $Z(\varepsilon)$ is therefore the cyclicity of the closed period annulus $\bar{\Pi}_\varepsilon$ with respect to the deformed foliation $\mathcal{F}_{\varepsilon,\delta}$ [10]. The purpose of the paper is to prove the ε-uniform boundedness of $Z(\varepsilon)$ in the case when the slow-fast foliation $\mathcal{F}_\varepsilon$ has a Darboux type first integral H of the form

$$H = (y - x^2)^\varepsilon (1 - y).$$

Another motivation for our result comes from the program of proving uniform finiteness of the number of limit cycles of plane quadratic vector fields [7, 10] (the existential Hilbert's 16th problem). Indeed, a family of plane quadratic systems can be slow-fast, with a first integral as above, and with degenerate graphics; see Figure 1.1.

The main difficulty in the study of $\mathcal{F}_{\varepsilon,\delta}$ is on the one hand the neighborhood of the "turning point" $(0, 0)$ of $\mathcal{F}_0$, and on the other hand the double heteroclinic loop $\{y = x^2\}$ of $\mathcal{F}_\varepsilon$ $(\varepsilon > 0)$. The zeros of pseudo-Abelian integrals appearing in the usual Poincaré-Melnikov method does not detect the so-called alien limit cycles [5]. Nevertheless, in recent papers [1, 2], it has been shown that the number of zeros of pseudo-Abelian integrals, which arise as a first approximation of the first return map of our slow-fast system, have the desired uniform finiteness property.

In this paper we replace the pseudo-Abelian integrals, associated to $\mathcal{F}_{\varepsilon,\delta}$ and studied in [1, 2], by the true Dulac maps defining the limit cycles as fixed points.

Received by the editors September 13, 2013 and, in revised form, October 13, 2014.
2010 *Mathematics Subject Classification.* Primary 34C08, 34M03, 34M35.
Key words and phrases. Slow-fast system, limit cycle, double heteroclinic loop.
This research was supported by Polish NCN Grant No 2011/03/B/ST1/00330.

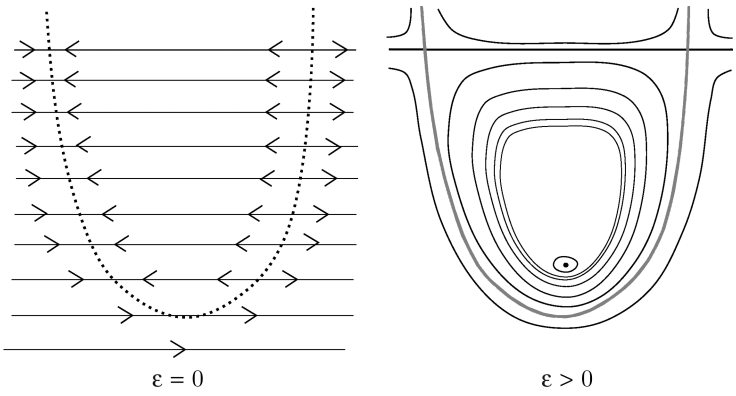

FIGURE 1.1. The slow-fast Darboux foliation $\mathcal{F}_\varepsilon$.

Our main result is the uniform finiteness of the number of limit cycles of the slow-fast Darboux system under consideration. The analytic deformations $\mathcal{F}_{\varepsilon,\delta}$ which we consider are arbitrary and can depend on an arbitrary given number of parameters.

Our method makes strong use of the properties of the foliation $\mathcal{F}_{\varepsilon,\delta}$ in a complex domain, where we apply a technique derived from the so-called "Petrov trick", along the lines of [8, 9].

Remark 1.1. Limit cycles of slow-fast foliations $\mathcal{F}_{\varepsilon,\delta}$ can be studied in the general framework of the method of slow-fast divergent integrals, developed by Dumortier, Roussarie (see [3, 4] and others). Such an approach reveals the existence of "canard limit cycles", but cannot capture all of the limit cycles of the foliation. The slow-fast divergent integrals cannot detect the limit cycles which tend to the big separatrix polycycle, when $\varepsilon, \delta \to 0$. Similarly, there are also limit cycles tending to the turning point; see the recent paper [6] on this subject.

On the other hand, the divergence integral method can detect and locate the canard limit cycles in a more accurate way. The difference of these two methods is presented in Figure 1.2. Our method covers a narrow region around the integrable direction which is the ε-axis, while the slow-fast technique covers a narrow region around the canard manifold. If the parameter δ is appropriately chosen, then the canard curve is the δ-axis; see Figure 1.2.

Nevertheless, it would be interesting to compare these two methods, but this is definitely beyond the scope of this paper.

Remark 1.2. We tried to make the paper as self-contained as possible, but we used quite essentially some ideas from papers [2, 8, 9]. To help the reader we recall below the main ideas used. The key point of the papers [8, 9] is the observation that the Dulac map along the non-degenerate saddle has analytic continuation to the complex domain and the *real* locus (i.e., the set where the imaginary part vanishes) is a smooth analytic curve up to the origin. The key point of the paper [2] is the iterated variation technique applied to the slow-fast systems. The geometric variation of the integrable trajectory allows us to avoid the slow manifold. This idea combined with the blow-up in extended phase-space gives the upper bound for the limit cycles bifurcating the slow-fast integrable system.

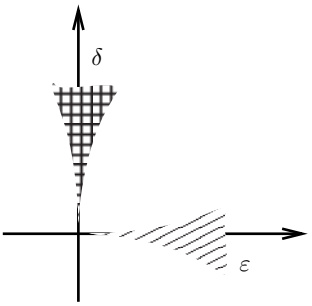

FIGURE 1.2. Dashed region of parameters covered by the paper, the slow-fast part marked by net.

2. Statement of the result

Using the notation of [2], let $P_0 = P_0(x,y), P_1 = P_1(x,y)$ be real bivariate polynomials and consider the differential system

$$P_1' = \varepsilon P_1, \quad P_0' = -P_0, \ \ \varepsilon \in \mathbb{R}^+, \tag{2.1}$$

which induces the foliation

$$\mathcal{F}_\varepsilon : \varepsilon P_1 dP_0 + P_0 dP_1 = 0. \tag{2.2}$$

It has a Darboux type first integral

$$H = P_0^\varepsilon P_1,$$

and for $\varepsilon = 0$ a curve of singular points $\{(x,y) : P_0(x,y) = 0\}$. For ε close to zero the curve is the slow manifold of the slow-fast system (2.1).

In the present paper we are interested in the simplest possible slow-fast Darboux system, shown in Figure 1.1. More precisely, assume that

$$P_0 = y - x^2, \ P_1 = 1 - y.$$

Consider further the following perturbed slow-fast Darboux integrable foliation

$$\mathcal{F}_{\varepsilon,\delta} : \varepsilon P_1 dP_0 + P_0 dP_1 + P\mathrm{d}x + Q\mathrm{d}y = 0, \tag{2.3}$$

where $P = P(x,y,\delta)$, $Q = Q(x,y,\delta)$ are real polynomials in x, y depending analytically on $\delta \in (\mathbb{R}^N, 0)$, and such that

$$P(x,y,0) = Q(x,y,0) \equiv 0.$$

Alternatively, we may consider the vector field $X_{\varepsilon,\delta}$ underlying the foliation $\mathcal{F}_{\varepsilon,\delta}$:

$$X_{\varepsilon,\delta} : \left\{ \begin{array}{rcl} \dot{x} & = & y - x^2 - \varepsilon + \varepsilon y - Q(x,y,\delta), \\ \dot{y} & = & -2\varepsilon x + 2\varepsilon xy + P(x,y,\delta). \end{array} \right. \tag{2.4}$$

For every fixed sufficiently small $\varepsilon > 0$, denote by $Z(\varepsilon)$ the maximal number of limit cycles of $\mathcal{F}_{\varepsilon,\delta}$, which bifurcate from the compact region $\bar{\Pi}$ bounded by the curves $\{P_0 = 0\}$, $\{P_1 = 0\}$, for sufficiently small $\|\delta\|$. The number $Z(\varepsilon)$ is therefore the cyclicity of the closed period annulus $\bar{\Pi}$ of $\mathcal{F}_{\varepsilon,0}$ under the deformation $\mathcal{F}_{\varepsilon,\delta}$. The main result of the paper is the following theorem.

Theorem 2.1. *The cyclicity $Z(\varepsilon)$ is finite and uniformly bounded in $\varepsilon > 0$.*

Remark 2.2. We expect that Theorem 2.1 remains true under the following more general assumptions on the unperturbed Darboux integrable foliation (2.2).

Let P_0, P_1 be analytic functions, such that the real curves $\{P_0 = 0\}$, $\{P_1 = 0\}$ are smooth, intersect transversally, and bound a compact region $\overline{\Pi}$ in which the foliation (2.2) *has no singular points. The curve $\{P_0 = 0\}$ is, moreover, transverse to the foliation $dP_1 = 0$.*

3. The integrable foliation $\mathcal{F}_{\varepsilon,0}$ where $\varepsilon > 0$

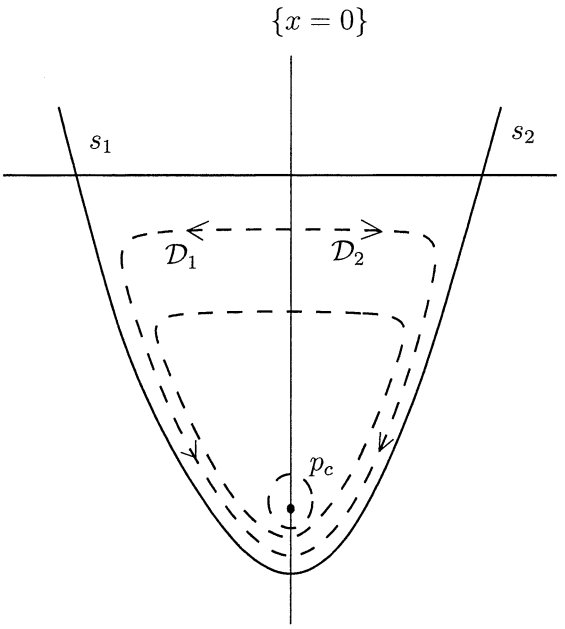

FIGURE 3.1. The real integrable plane foliation $\mathcal{F}_{\varepsilon,0}$ for $\varepsilon > 0$.

In this section we assume that $\delta = 0$ and $\varepsilon > 0$ is a sufficiently small fixed real parameter. The foliation $\mathcal{F}_{\varepsilon,0}$ has a Darboux type first integral $H = (y-x^2)^\varepsilon(1-y)$ and its phase portrait is shown in Figure 3.1. It has a real nest of cycles bounded by the parabola $y - x^2 = 0$ and a line $y - 1 = 0$. The center point is located at

$$p_c = (0, y_c),\ y_c = \tfrac{\varepsilon}{\varepsilon+1}.$$

3.1. **The complex leaves of $\mathcal{F}_{\varepsilon,0}$.** The leaves of dimension one of $\mathcal{F}_{\varepsilon,0}$ are connected open Riemann surfaces, on which the function

$$(y - x^2)^\varepsilon(1 - y)$$

is constant. Every leaf intersects the cross-section $\{x = 0\}$ at at least one point $(0, y_0)$. The Riemann surface C_ε of the multi-valued analytic function

$$f(y) := y(1 - y)^{1/\varepsilon},\ y \neq 1, \tag{3.1}$$

is conformally equivalent either to $\mathbb{C}$ ($\varepsilon \notin \mathbb{Q}$), or to $\mathbb{C}^*$ ($\varepsilon \in \mathbb{Q}$), and on the leaf through $(0, y_0)$

$$x^2 = (f(y) - f(y_0))(1 - y)^{-1/\varepsilon} \tag{3.2}$$

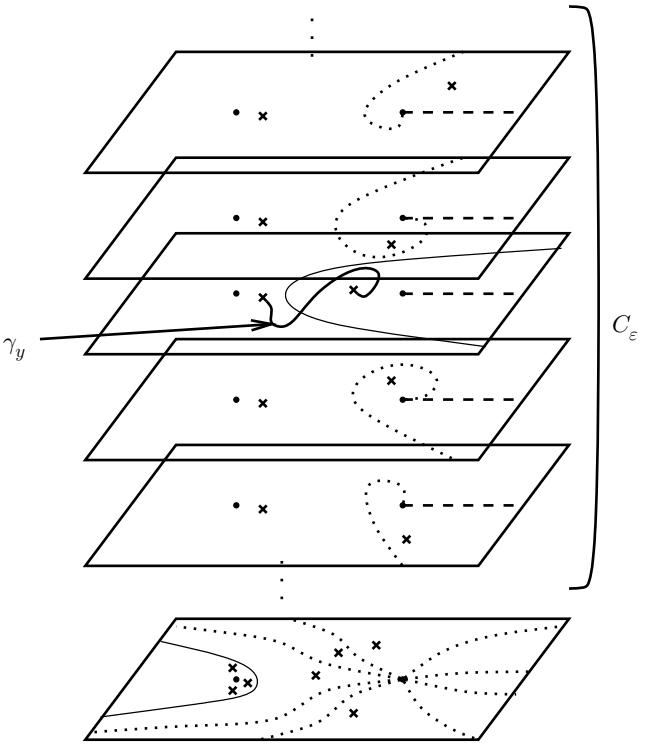

FIGURE 3.2. Every complex leaf of the foliation $\mathcal{F}_{\varepsilon,0}$, which is not the line $\{y = 1\}$, is a double covering of the Riemann surface C_ε.

holds. This implies the following.

Proposition 3.1. *Every complex leaf of the integrable foliation $\mathcal{F}_{\varepsilon,0}$ which does not contain the center point $(0, y_c)$, or is not the line $\{y = 1\}$, is a double covering of C_ε given by the formula* (3.2)*. The y-coordinates of the ramification points of the covering are the solution of the equation $f(y) = f(y_0)$. The leaf of $\mathcal{F}_{\varepsilon,0}$ through the center point $p_c = (0, y_c)$ has a single singular point at p_c which is a normal crossing, and otherwise is a double covering of C_ε given by the formula* (3.2)*, with ramification points $(0, y)$ satisfying $f(y) = f(y_c)$.*

3.2. **Analytic continuation of the Dulac maps.** Consider the cross-section $\{x = 0\}$ parameterized by y, as well the two Dulac maps $\mathcal{D}_1 = \mathcal{D}_2$

$$\mathcal{D}_{1,2} : (y_c, 1) \to (0, y_c), \tag{3.3}$$

shown in Figure 3.1. One obvious extension of $\mathcal{D}_{1,2}$ is

$$\mathcal{D}_{1,2} : (0, 1) \to (0, 1), \tag{3.4}$$

which is a real-analytic involution

$$\mathcal{D}_{1,2}(\bar{y}) = \overline{\mathcal{D}_{1,2}(y)}, \quad \mathcal{D}_{1,2}^2 = id, \quad \mathcal{D}_{1,2}(p_c) = p_c.$$

For the needs of the present paper we do not need a global description of the Dulac maps, but only an appropriate domain of analyticity in which we shall later apply the argument principle. This domain is described as follows.

Let $C_{\pm\pi}$, $C_{\pm 0}$ be the real curves in the complex y-plane, defined in polar coordinates as

$$C_{+0} = \{\rho = \frac{\sin(\varepsilon\varphi)}{\sin(\varphi+\varepsilon\varphi)} : -\frac{\pi}{1+\varepsilon} < \varphi < \frac{\pi}{1+\varepsilon}\},$$
$$C_{-0} = \{\rho = \frac{\sin(\varepsilon\varphi)}{\sin(\varphi+\varepsilon\varphi)} : 0 < \varphi < \frac{\pi}{1+\varepsilon}\},$$
$$C_{-\pi} = \{\rho = \frac{\sin(\varepsilon\varphi+\varepsilon\pi)}{\sin(\varphi+\varepsilon\varphi+\varepsilon\pi)} : 0 < \varphi < \frac{\pi(1-\varepsilon)}{1+\varepsilon}\},$$
$$C_{\pi} = \{\rho = \frac{\sin(\varepsilon\varphi-\varepsilon\pi)}{\sin(\varphi+\varepsilon\varphi-\varepsilon\pi)} : -\frac{\pi(1-\varepsilon)}{1+\varepsilon} < \varphi < 0\}.$$

Let $\mathbf{D}_1$ be the open complex domain delimited by the curves $C_{\pm 0}$ and $C_{\pm\pi}$, and let $\mathbf{D}_0$ be the complex domain delimited by the curves $C_{\pm 0}$ and the segment $(-\infty, 0)$; see Figure 3.3.

Proposition 3.2. *The real Dulac maps* (3.4) *allow an extension to biholomorphic maps*

$$\mathcal{D}_{1,2} : \mathbf{D}_0 \cup \mathbf{D}_1 \cup C_{+0} \cup C_{-0} \cup \{y_c\} \to \mathbf{D}_0 \cup \mathbf{D}_1 \cup C_{+0} \cup C_{-0} \cup \{y_c\},$$

where

$$\mathcal{D}_{1,2}(\mathbf{D}_1) = \mathbf{D}_0,\ \mathcal{D}_{1,2}(C_{+0}) = C_{-0}, \mathcal{D}_{1,2}(y_c) = y_c.$$

They can be further analytically continued to a suitable open neighborhood of C_π, $C_{-\pi}$, and

$$\mathcal{D}_{1,2}(C_{-\pi}) = \mathcal{D}_{1,2}(C_\pi) = (-\infty, 0).$$

The limit of $\mathcal{D}_{1,2}$ at $y = 1$ exists and $\mathcal{D}_{1,2}(1) = 0$.

Proof. The function $H(0, y) = y^\varepsilon(1-y)$ allows an analytic continuation in $\mathbb{C} \setminus (-\infty, 0]$. The real Dulac map satisfies $H(0, y) = H(0, \mathcal{D}_{1,2}(y))$ and so does its complex extension, when it exists. Consider the isoclines

$$C_\theta = \{y \in \mathbf{D}_0 \cup \mathbf{D}_1 : \arg(y^\varepsilon(1-y)) = \varepsilon\theta\},$$

or equivalently

$$C_\theta = \{y : \varepsilon \arg(y) + \arg(1-y) = \varepsilon\theta\},$$

which implies in polar coordinates

$$C_\theta = \{(\rho, \phi) : \rho = \frac{\sin(\varepsilon\varphi-\theta)}{\sin(\varphi+\varepsilon\varphi-\theta)}\}.$$

Thus $\mathbf{D}_1 \cup \mathbf{D}_0$ is a union of the isoclines C_θ:

$$\mathbf{D}_1 \cup \mathbf{D}_0 = \{C_\theta : -\pi < \theta < \pi\},$$

where each C_θ has exactly two connected components, contained respectively in $\mathbf{D}_1$ or $\mathbf{D}_0$; see Figure 3.3. For $\theta = 0$ the Dulac map exchanges the segments $(0, y_c)$ and $(y_c, 1)$; by continuity the same holds true for all θ. Moreover, by a local analysis of the Dulac map near 1 we have

$$\lim_{y\to 1} \mathcal{D}_{1,2}(y) = 0,$$

and the identity $|y^\varepsilon(1-y)| = |\mathcal{D}_{1,2}(y)^\varepsilon(1-\mathcal{D}_{1,2}(y))|$ implies that when $|y|$ tends to infinity along C_θ, then so does $\mathcal{D}_{1,2}(y)$. As $\mathcal{D}'_{1,2}(y) \neq 0$, then $\mathcal{D}_{1,2}$ is a bianalytic map between connected components of C_θ, a bijection between $\mathbf{D}_1$ and $\mathbf{D}_0$, and finally a biholomorphic map between $\mathbf{D}_1$ and $\mathbf{D}_0$. The claims about the behavior of $\mathcal{D}_{1,2}$ along the border of the domains $\mathbf{D}_1$, $\mathbf{D}_0$ are straightforward. □

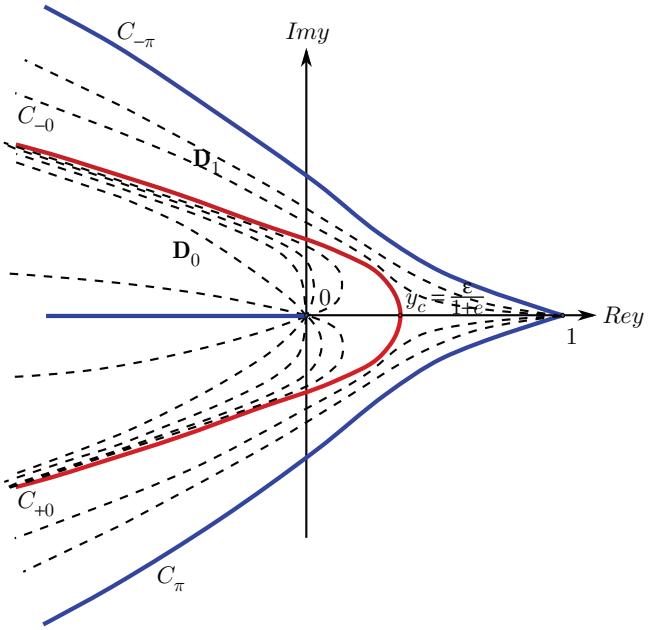

FIGURE 3.3. The isoclines of the function $y^\varepsilon(1-y)$

Consider the continuous family of orbits $\{\gamma_y^{1,2}\}_y$, $y \in (\varepsilon/(1+\varepsilon), 1)$, defining $\mathcal{D}_{1,2}(y)$ in Figure 3.1 respectively. Each $\gamma_y^{1,2}$ is a real path starting at y and terminating at $\mathcal{D}_{1,2}(y)$.

Definition 3.3. We shall say that the analytic functions $\mathcal{D}_{1,2}$ defined in the domain $\mathbf{D}_1$ allow a geometric realization, provided that the continuous families of real paths $\{\gamma_y^{1,2}\}_y$, $y \in (y_c, 1)$, allow an extension to continuous families of paths $\{\gamma_y\}_{y\in\mathbf{D}_1}$, contained in the complex leaves of the foliation $\mathcal{F}_{\varepsilon,0}$, such that each $\gamma_y^{1,2}$ starts at y and terminates at $\mathcal{D}_{1,2}(y)$.

Of course, the families of paths $\{\gamma_y\}_y$ are defined up to a homotopy. We note that although $\mathcal{D}_1 = \mathcal{D}_2$ they allow non-equivalent geometric realizations.

Proposition 3.4. *The real Dulac maps $\mathcal{D}_{1,2}$ allow a geometric realization in the domain $\mathbf{D}_1$.*

Proof. Consider the projection

$$\pi : \mathbb{C} \to \mathbb{C} : (x, y) \mapsto y,$$

and let Γ_y be the connected component of a leaf of the foliation $\mathcal{F}_{\varepsilon,0}$ through the point $(0, y)$ which is contained in the pre-image under π of the domain $\overline{\mathbf{D}}_0 \cup \mathbf{D}_1$. If $c = y^\varepsilon(1-y)$, then along Γ_y

$$x^2 = y + c(1-y)^{-\frac{1}{\varepsilon}} \tag{3.5}$$

holds, which shows that $\pi : \Gamma_y \to \overline{\mathbf{D}}_0 \cup \mathbf{D}_1$ is a double covering, ramified at the points y and $\mathcal{D}_1(y) = \mathcal{D}_2(y)$. The leaf Γ_y is therefore a smooth open Riemann surface, except Γ_{y_c}, which has a normal crossing at $(0, y_c)$, where $y_c = \mathcal{D}_1(y_c) = \mathcal{D}_2(y_c)$.

Let σ_y be a path in $\overline{\mathbf{D}}_0 \cup \mathbf{D}_1$ connecting y to $\mathcal{D}_1(y) = \mathcal{D}_2(y)$. Such a path can be lifted in Γ_y under π in two different ways. To every continuous family of paths σ_y correspond therefore two continuous families of lifts in $\gamma_y \subset \Gamma_y$. We now apply these considerations to the continuous family of segments $\sigma_y = [y, \mathcal{D}_{1,2}(y)] \subset \mathbb{R}$, $y \in (y_c, 1)$. The lift of σ_y will be the real orbit γ_y^1 or γ_y^2 defining $\mathcal{D}_1(y)$ or $\mathcal{D}_2(y)$, and shown in Figure 3.1.

To complete the proof:

- First extend, the segments $\sigma_y = [y, \mathcal{D}(y)] \subset \mathbb{R}$ to a continuous family of paths $\sigma_y \subset \mathbf{D}_1 \cup \mathbf{D}_0$, $y \in \mathbf{D}_1$ which connect $y \in \mathbf{D}_1$ to $\mathcal{D}(y) \in \mathbf{D}_0$, as is illustrated in Figure 3.4.

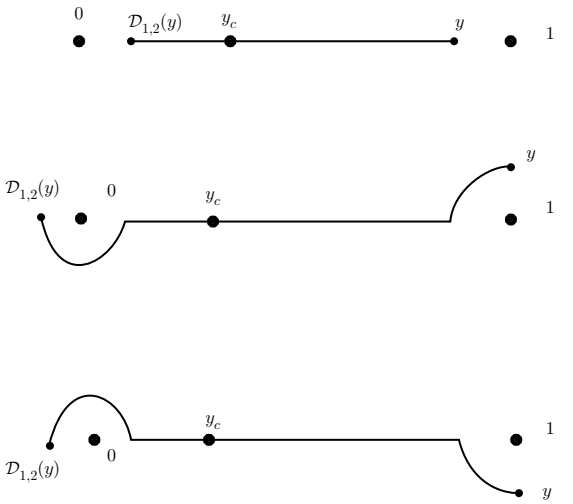

FIGURE 3.4. The continuous family of paths $\{\sigma_y\}_y$.

- Second, to each path σ_y, $y \in \mathbf{D}_1$, we associate its lift γ_y with respect to π with initial point $(0, y)$. For $y \in (y_c, 1)$ the lift γ_y was already defined, by continuity it will be defined without ambiguity for all $y \in \mathbf{D}_1$. For $y \in (y_c, 1)$ the end point of γ_y is $(0, \mathcal{D}(y))$. As the end point of γ_y depends analytically on y, then it is $(0, \mathcal{D}(y))$ for all $y \in \mathbf{D}_1$. □

Remark 3.5. The above considerations show that the Riemann surface Γ_y is a topological cylinder, which is a double covering of the topological disc $\overline{\mathbf{D}}_0 \cup \mathbf{D}_1$, ramified over y and $\mathcal{D}(y)$. The closed loop $\gamma_y^1 \circ (\gamma_y^2)^{-1}$ is the generator of the fundamental group of the cylinder.

Remark 3.6. It can be shown by making use of Proposition 3.1 that $\mathcal{D}_{1,2}$ also allows an analytic extension to $\mathbb{C} \setminus \{1\}$ with countably many algebraic singularities. More precisely, if $y_0 \neq 1$ is a singular point, then y_0 belongs to the leaf through the center point p_c. The curve on the y-plane containing the possible singular points is defined therefore by the equation

$$\{y : |f(y)| = |f(y_c)|\}.$$

This curve is easily analyzed and it is shown in Figure 3.5.

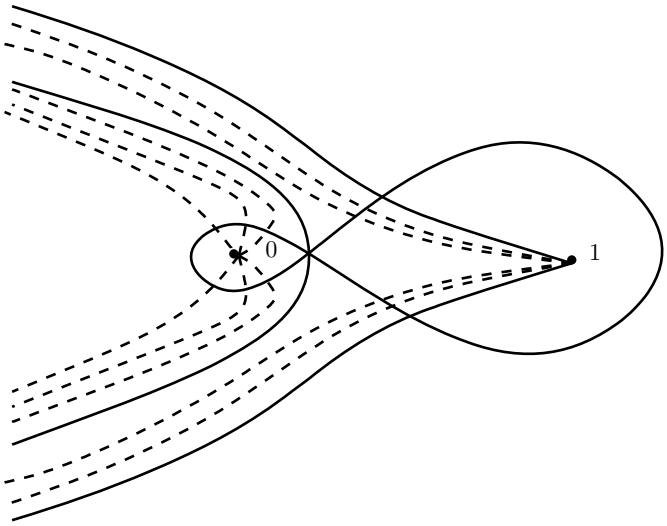

FIGURE 3.5. The curve $\{y : |f(y)| = |f(y_c)|\}$.

3.3. **Geometric variation.** We describe a geometric construction of the variation. It will be used later to control intersection points of curves $\{Im\mathcal{D}_1 = 0\}$ and $\{Im\mathcal{D}_2 = 0\}$.

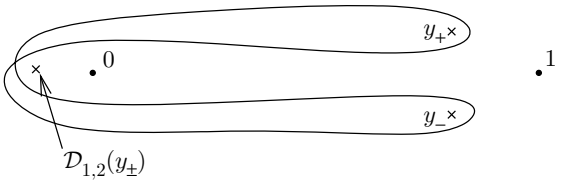

FIGURE 3.6. Projection of the figure-eight loop γ_8 to the $x = 0$ transversal.

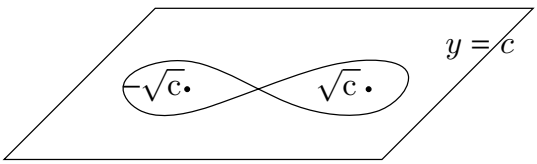

FIGURE 3.7. The figure-eight loop γ_8 at the limit $\varepsilon \to 0$.

In the following proposition a dot denotes the product in the path groupoid, i.e., $\gamma^1 \cdot \gamma^2$ denotes the path consisting of γ^1 followed by γ^2, where the end point of γ_1 coincides with the starting point of γ_2, the analog meaning for the inverse.

Proposition 3.7. *Let $\gamma_y^{1,2}$ be a geometric realization of the Dulac maps $\mathcal{D}_{1,2}$ and let $y_\pm \in C_{\pm\pi}$ and $y_- = \overline{y_+}$. The path $\gamma_8 = (\gamma^1_{y_+} \cdot (\gamma^2_{y_-})^{-1}) \cdot \overline{(\gamma^1_{y_+} \cdot (\gamma^2_{y_-})^{-1})}$ is a closed loop that projects on the y-plane to the loop shown in Figure* 3.6. *It can be*

homotopically deformed to a loop located a finite (ε-independent) distance from the slow parabola $y - x^2 = 0$. At the limit $\varepsilon \to 0$ it is the figure-eight loop in the leaf of fast foliation; see Figure 3.7.

Proof. By definition of the curves $C_{\pm\pi}$, $\mathcal{D}_{1,2}(y_\pm) \in \mathbb{R}_-$; due to the conjugation relation $y_- = \overline{y_+}$ and the Schwartz reflection principle, the images of $y_\pm$ coincide. Thus, the path $(\gamma^1_{y_+} \cdot (\gamma^2_{y_-})^{-1})$ joins Y_+ with y_- and passes through the third ramification point $\mathcal{D}_{1,2}(y_\pm)$ of the double covering (3.5). It can be deformed homotopically to the path avoiding the ramification point $\mathcal{D}_{1,2}(y_\pm)$ from the left.

The next path is a complex conjugacy of the first one. It is the same composition of γ paths with indices $(1, 2)$ exchanged and the direction reversed. The composition is as shown in Figure 3.6 after homotopical deformation that avoids the ramification points $y_\pm$. □

4. Blowing up the turning point

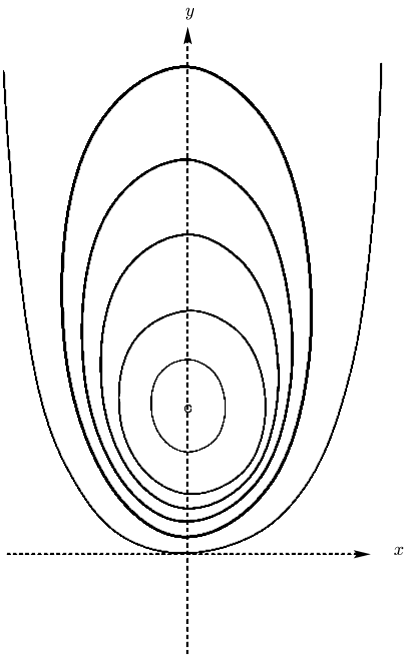

FIGURE 4.1. The real level sets of $e^{-y}(y - x^2)$.

When ε tends to zero, the center p_c of the integrable foliation tends to the contact point $p_0 = (0, 0)$ of the slow manifold $\{y = x^2\}$ with the leaves $y = const$. The point p_0 is therefore the turning point of our slow-fast Darboux foliation $\mathcal{F}_{\varepsilon,0}$, and the study of the Dulac map near p_0 when ε tends to zero will be studied, as explained in detail in [2, section 3], by a weighted blow-up in the (x, y, ε)-space. Namely, the rescaling

$$x \to \sqrt{\varepsilon}x,\ y \to \varepsilon y,\ \varepsilon \to \varepsilon, \tag{4.1}$$

sends the center point y_c to $1/(1+\varepsilon)$, leaves the parabola $y = x^2$ invariant, and transforms the first integral $[(1-y)(y-x^2)^{\varepsilon}]^{1/\varepsilon}$ of the foliation $\mathcal{F}_{\varepsilon,0}$ to the form

$$\varepsilon(1-\varepsilon y)^{\frac{1}{\varepsilon}}(y-x^2) = \varepsilon e^{-y+O(\varepsilon)}(y-x^2) = \varepsilon e^{-y}(y-x^2) + O(\varepsilon^2).$$

The blown-up foliation has therefore, in every compact neighborhood of the origin, an analytic first integral, uniformly in x, y, $O(\varepsilon)$-close to

$$e^{-y}(y-x^2);$$

see Figure 4.1. Finally, the curves $C_{\pm\pi}$ are transformed to curves on a finite distance from the origin $y = 0$; see Figure 4.2.

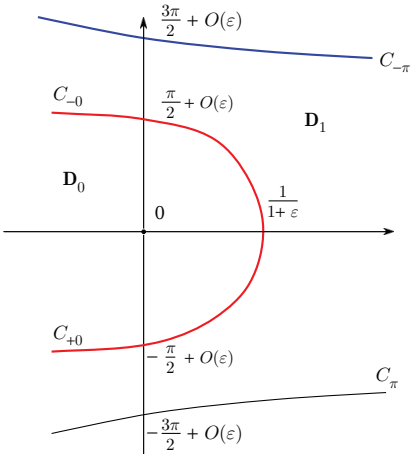

FIGURE 4.2. The cross-section $\{x = 0\}$ in a neighborhood of the turning point after the weighted blow-up of the (x, y, ε)-space.

5. The perturbed foliation $\mathcal{F}_{\varepsilon,\delta}$ where $\varepsilon > 0$ and $\|\delta\|$ is much smaller than ε

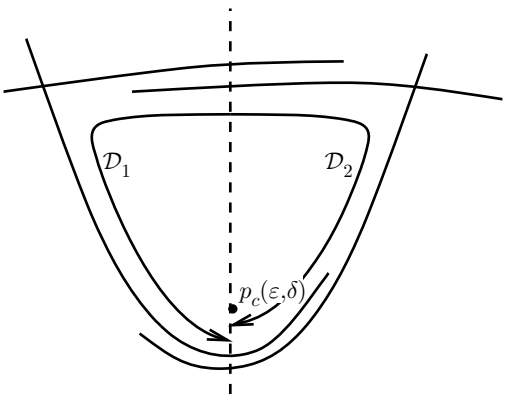

FIGURE 5.1. Two Dulac maps for the perturbed system.

In the preceding section we considered two Dulac maps $\mathcal{D}_1$ and $\mathcal{D}_2$ which coincide as analytic functions, but were defined geometrically in two different ways. We have respectively two non-equivalent geometric realizations $\{\gamma_y^{1,2}\}_{y\in\mathbf{D}_1}$ of the same analytic function $\mathcal{D} = \mathcal{D}_1 = \mathcal{D}_2$. In this section we suppose that $\varepsilon > 0$ is fixed, $\delta \in \mathbb{R}^N$, and $\|\delta\|$ is sufficiently small with respect to ε. Let $p_c = (x_c, y_c)$ be the singular point (a focus) of $\mathcal{F}_{\varepsilon,\delta}$, close to the center of $\mathcal{F}_{\varepsilon,0}$. We consider the cross-section $\{x = x_c\}$ and as before define geometric realizations of the corresponding Dulac maps $\mathcal{D}_1$ and $\mathcal{D}_2$. Indeed, when $\delta \neq 0$, the continuous family of paths $\{\gamma_y^{1,2}\}_{y\in\mathbf{D}_1}$, contained in the leaves of the foliation $\mathcal{F}_{\varepsilon,0}$, persist under a small perturbation, at least when the initial point $(0, y)$ belongs to a relatively compact domain $K\cup\mathbf{D}_1$, and the leaves of the foliation $\mathcal{F}_{\varepsilon,0}$ are transverse to the line $\{x = 0\}$ at $(0, y)$, as well as at $(0, \mathcal{D}(y))$. We obtain in this way two continuous families of paths in the leaves of the perturbed foliation $\mathcal{F}_{\varepsilon,\delta}$, which begin at a point $(0, y)$ and terminate at a point $(0, \mathcal{D}^1(y)$ or $(0, \mathcal{D}^2(y)$ respectively.

The above also holds true in a neighborhood of the center point p_c (which becomes a focus after the perturbation), but also in a neighborhood of the singular point $(0, 1) \in \{x = 0\}$. Indeed, after the perturbation a saddle point persists, and the Dulac map near such a point is defined in every fixed sector, centered at the singular point. The image of the real analytic curves $C_{\pm\pi}$ under the Dulac map is the negative real semi-axes; see Proposition 3.2. Therefore these curves can also be defined by the condition that $\{y : Im(\mathcal{D}^1(y)) = 0$ and $Im(\mathcal{D}^2(y)) = 0$. We denote for a further use these two curves by $C^1_{\pm\pi} = C^1_{\pm\pi}(\varepsilon, \delta)$ and $C^2_{\pm\pi} = C^2_{\pm\pi}(\varepsilon, \delta)$, respectively (when there is no ambiguity, the dependence on ε and δ is omitted).

As shown in [8, 9], the curves $C^{1,2}_{\pm\pi}$ are analytic, including at the singular points of the Dulac maps, corresponding to the saddles s_1 and s_2. Consider the closed

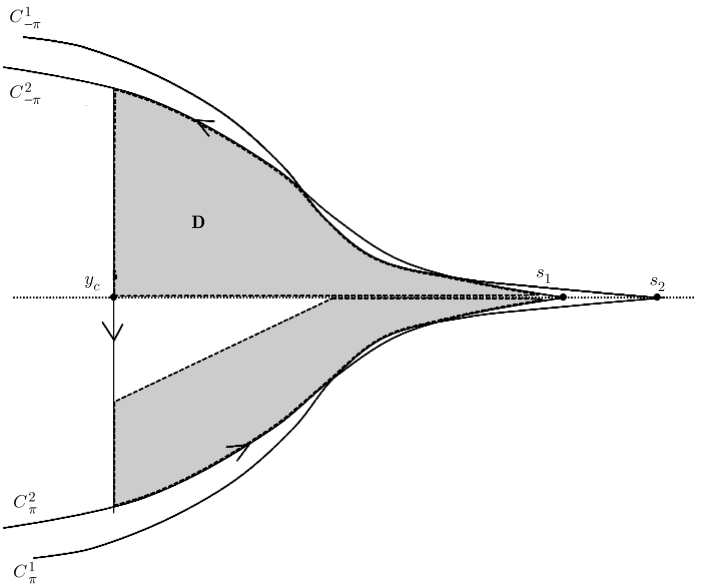

FIGURE 5.2. The complex domain $\mathbf{D}$, bounded by $C^{1,2}_{\pm\pi}$, and the line $\mathcal{R}e\ y > y_c$.

complex domain $\mathbf{D}$, which is bounded by $C^{1,2}_{\pm\pi}$, and the line $\mathcal{R}e\ y > y_c$, as in Figure 5.2.

Proposition 5.1. *The number of the limit cycles of $\mathcal{F}_{\varepsilon,\delta}$, bifurcating from the closed period annulus of $\mathcal{F}_{\varepsilon,0}$ is bounded by the variation of the argument of the analytic function $\mathcal{D}_1 - \mathcal{D}_2$ divided by 2π along the border $\partial\mathbf{D}$ of the domain shown in Figure* 5.2.

Proof. The Dulac maps have analytic continuations in $\mathbf{D}$, as their geometric realizations persist under sufficiently small perturbation. The limit cycles are in a one-to-one correspondence with the fixed points y, $\mathcal{D}_1(y) = \mathcal{D}_2(y)$ of the first return map. Therefore it is enough to bound the zeros of $\mathcal{D}_1 - \mathcal{D}_2$ by making use of the argument principle, as explained in [9, Section 2.1]. □

Corollary 5.2. *For every fixed $\varepsilon > 0$ and for every sufficiently small δ, the Dulac maps $\mathcal{D}_1, \mathcal{D}_2$ are real analytic functions in a suitable neighborhood of $\mathbf{D} \setminus \{s_i\}$ where $s_i \sim 1$ are the singular points of the Dulac maps.*

Our intention is to apply the argument principle to the analytic function $\mathcal{D}_1 - \mathcal{D}_2$ in $\mathbf{D}$ in order to bound its complex zeros (equivalently, fixed points of the return map, or complex limit cycles). For this we note that although the Dulac map is singular at s_i, it is continuous at these points. We shall bound uniformly on one side, the variation of the argument of $\mathcal{D}_1 - \mathcal{D}_2$ along the segment $\{\mathcal{R}e\ y > y_c\} \cap \mathbf{D}$, and on the other hand the number of the zeros of the imaginary part of $\mathcal{D}_1 - \mathcal{D}_2$ along $\{C_1^{\pm} \cup C_2^{\pm}\} \cap \mathbf{D}$. By definition of the curves $C_1^{\pm}, C_2^{\pm}$, these zeros are just the intersection points $C_1^{+} \cap C_2^{+}+$ and $C_1^{-} \cap C_2^{-}$, counted with multiplicity. The curves $C_1^{\pm}, C_2^{\pm}$ depend, however, on ε, δ, and their behavior when the parameters ε, δ tend to zero is crucial. When $\delta = 0$, $\varepsilon > 0$ the curves are explicit and tend to the real axes as $\varepsilon \to 0$.

6. Proof of Theorem 2.1

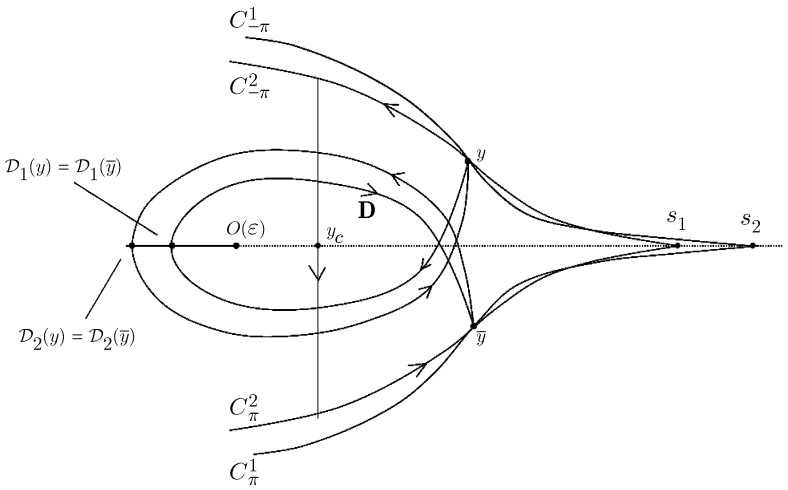

FIGURE 6.1. The geometric realization of the holonomy $\mathcal{H}ol$ and its projection on the cross-section.

Suppose first that $\varepsilon > 0$ belongs to a sufficiently small but fixed neighborhood of the origin. Consider first the segment corresponding to the part of $\partial\mathbf{D}$ contained in the line $\{\mathcal{R}e\ y = y_c\}$. It follows from Proposition 3.4 that along this segment the functions $\mathcal{D}_1$, $\mathcal{D}_2$ have a geometric realization and hence are analytic, both in y and ε, δ, provided that $\varepsilon \neq 0$ and $\|\delta\|$ is much smaller than ε. To prove the analyticity in a neighborhood of $\varepsilon = 0$ we consider the rescaling (4.1) and the domain $\mathbf{D}_1$ shown in Figure 4.2. It can be shown along the same lines as in Proposition 3.4 that the Dulac maps have a geometric realization in $\mathbf{D}_1$ again, and hence it is also analytic in $\sqrt{\varepsilon}, \delta$, in a neighborhood of $\varepsilon = 0, \delta = 0$. This implies the analyticity for ε, δ close to zero (after the rescaling). Therefore the variation of the argument along the compact segment, corresponding to the part of $\partial\mathbf{D}$, contained in the line $\{\mathcal{R}e\ y = y_c\}$, is uniformly bounded.

Along the remaining part of $\partial\mathbf{D}$ the displacement map $\mathcal{D}_1 - \mathcal{D}_2$ is analytic, except at the singular points s_i. For this purpose we bound the increase of the argument of $\mathcal{D}_1 - \mathcal{D}_2$ by the number of the zeros of its imaginary part (the so-called "Petrov trick") along $\partial\mathbf{D}$. Clearly, these zeros are exactly the intersection points of the curves $\{Im\ \mathcal{D}_1 = 0\}$, $\{Im\ \mathcal{D}_2 = 0\}$, that is to say $C^1_{-\pi} \cap C^2_{-\pi}$ and $C^1_{+\pi} \cap C^2_{+\pi}$. The intersection points have a transparent geometric meaning: they correspond to complex limit cycles intersecting the cross-section, or fixed points of the holonomy map $\mathcal{H}ol$ along the "figure-eight loop" which we recall now (see [2, 8, 9]). If the holonomy map $\mathcal{H}ol$ were analytic with respect to the parameters too, this would imply a uniform bound for the number of fixed points, and hence completes the proof of the theorem.

The one-dimensional leaves of the foliation $\mathcal{F}_{0,0}$ are the punctured discs $\{(x, y) : y = c\} \setminus \{(\pm\sqrt{c}, c)\}$, where $c \neq 0$. The geometric realization of $\mathcal{H}ol = id$ is then explained in Proposition 3.7 and shown in Figures 3.6, 3.7 from which the analyticity follows, except along the leaf $\{y = 0\}$ through the turning point $(0, 0)$. In a neighborhood of the turning point we use the rescaling (4.1) and describe the geometric realization of $\mathcal{H}ol$ as follows. Let $y \in C_{-\pi}$ in Figure 6.1 and note that $\bar{y} \in C_{+\pi}$. Consider the paths in the leaves of the foliation $\mathcal{F}_{0,0}$

$$\gamma^1_y, (\gamma^1_{\bar{y}})^{-1}, \gamma^2_y, (\gamma^2_{\bar{y}})^{-1},$$

connecting the points $y, \mathcal{D}_1(y), \bar{y}, \mathcal{D}_2(y), y$. These paths can be composed and the resulting closed path defines the holonomy map $\mathcal{H}ol$ which is then obviously analytic in ε, δ. The projection of these four paths on the cross-section, in the case of a fixed point of $\mathcal{H}ol$, are shown in Figure 6.1.

Acknowledgement

The authors thank the referee for helpful suggestions.

References

[1] Marcin Bobieński, Pavao Mardešić, and Dmitry Novikov, *Pseudo-Abelian integrals: unfolding generic exponential*, J. Differential Equations **247** (2009), no. 12, 3357–3376, DOI 10.1016/j.jde.2009.06.019. MR2571581 (2011c:37041)

[2] Marcin Bobieński, Pavao Mardešić, and Dmitry Novikov, *Pseudo-abelian integrals on slow-fast Darboux systems* (English, with English and French summaries), Ann. Inst. Fourier (Grenoble) **63** (2013), no. 2, 417–430. MR3112517

[3] Freddy Dumortier and Robert Roussarie, *Canard cycles and center manifolds*, Mem. Amer. Math. Soc. **121** (1996), no. 577, x+100, DOI 10.1090/memo/0577. With an appendix by Cheng Zhi Li. MR1327208 (96k:34113)

[4] Freddy Dumortier and Robert Roussarie, *Multiple canard cycles in generalized Liénard equations*, J. Differential Equations **174** (2001), no. 1, 1–29, DOI 10.1006/jdeq.2000.3947. MR1844521 (2002k:34076)

[5] Freddy Dumortier and Robert Roussarie, *Abelian integrals and limit cycles*, J. Differential Equations **227** (2006), no. 1, 116–165, DOI 10.1016/j.jde.2005.08.015. MR2233957 (2007c:34049)

[6] Freddy Dumortier and Robert Roussarie, *Birth of canard cycles*, Discrete Contin. Dyn. Syst. Ser. S **2** (2009), no. 4, 723–781, DOI 10.3934/dcdss.2009.2.723. MR2552119 (2010j:34124)

[7] F. Dumortier, R. Roussarie, and C. Rousseau, *Hilbert's 16th problem for quadratic vector fields*, J. Differential Equations **110** (1994), no. 1, 86–133, DOI 10.1006/jdeq.1994.1061. MR1275749 (95g:58179)

[8] Lubomir Gavrilov, *On the number of limit cycles which appear by perturbation of Hamiltonian two-saddle cycles of planar vector fields*, Bull. Braz. Math. Soc. (N.S.) **42** (2011), no. 1, 1–23, DOI 10.1007/s00574-011-0001-z. MR2774172 (2012b:34080)

[9] Lubomir Gavrilov, *On the number of limit cycles which appear by perturbation of Hamiltonian two-saddle cycles of planar vector fields*, Bull. Braz. Math. Soc. (N.S.) **42** (2011), no. 1, 1–23, DOI 10.1007/s00574-011-0001-z. MR2774172 (2012b:34080)

[10] Robert Roussarie, *Bifurcation of planar vector fields and Hilbert's sixteenth problem*, Progress in Mathematics, vol. 164, Birkhäuser Verlag, Basel, 1998. MR1628014 (99k:58129)

Institute of Mathematics, Warsaw University, ul. Banacha 2, 02-097 Warsaw, Poland
E-mail address: mbobi@mimuw.edu.pl

Institut de Mathématiques de Toulouse, UMR 5219, Université de Toulouse, CNRS, UPS IMT, F-31062 Toulouse Cedex 9, France